

An acousto-optic modulator based bi-frequency interferometer for quantum technology

Wenqi Li, Qiqi Deng, Xueshi Guo,^{*} and Xiaoying Li[†]
*College of Precision Instrument and Opto-Electronics Engineering,
Key Laboratory of Opto-Electronics Information Technology,
Ministry of Education, Tianjin University,
Tianjin 300072, People's Republic of China*

(Dated: October 4, 2022)

Acousto-optic modulators (AOMs) have been widely used in quantum optical technology, but the non-ideal diffraction efficiency limits its application in a quantum system. Here we experimentally demonstrate a bi-frequency interferometer scheme by using AOMs as the beam-splitter and the beam-combiner with a near perfect visibility of $(99.5 \pm 0.2)\%$. Chopped phase locking mode to arbitrary phase offset of the interferometer is achieved by directly introducing phase dithering to the splitting AOM. These features enable the interferometer functions as a high efficiency optical switch for quantum technology. Further discussion shows the interferometer can accomplish the coherent combination of quantum state with different optical frequency and is useful for the generation of entangled quantum state.

I. INTRODUCTION

Making use of acousto-optic bragg diffraction effect, Acousto-optic modulators (AOMs) are versatile active optical devices that can efficiently change both the frequency and the propagating direction of a laser beam in real time [1]. AOMs have been widely used in various applications, such as to stabilize the output power, to reduce the line-width and to shape the spatial profile of a laser beam [2–4]. Besides, AOMs can also realize active optical tweezers and ultra short pulse picking [5, 6].

AOMs are also indispensable devices in quantum optical technology. Due to its high isolation switching property, they are used in photon subtraction based Non-Gaussian state generation [7], photon triggered homodyne tomography [8] or controlling of a quantum memory [9]. Due to its frequency shifting property, AOMs are used to implement optical heterodyning [10, 11], to observe a beating from single photons [12] or to generate a phase locking reference without displacing the quantum state [13]. Current commercial AOMs have a diffraction efficiency larger than 85% per pass with the constrain of input beam size and driving power. While this efficiency is enough for most of the classical applications, it is still not high enough for the quantum applications where quantum states have to transmit through the AOMs and keep the high purity property, especially for those schemes that multiple diffraction passes are necessary [14, 15]. This impels us to consider the interferometric enhancement of the diffraction effect when using AOMs in quantum technology.

Interferometers with AOMs as important components have been demonstrated, but in most schemes AOMs are used to modulate one of the interferometer arm [16, 17]. In Ref. [11], an AOM is used as a beam-splitter to implement photon heterodyning. Recently, Ref. [12] reports an interferometer scheme using AOMs as the beam-splitter and the beam-combiner to observe the beating signal of single photons. However, the visibility of the interferometer in [12] is about 15%, which is not suitable for most efficiency sensitive quantum technology. Here we demonstrate an acousto-optic modulator based bi-frequency interferometer (ABI). By carefully designing the optical system and controlling the spatial mode of the two arms, we achieve a beating signal with a near perfect visibility of $(99.5 \pm 0.2)\%$. This high visibility feature enable us to achieve many quantum optical technology in a high quantum efficiency. Further, the interferometer can stably work in arbitrary phase with a dither phase locking system [18] in chopped locking mode, and the minimum locking duty cycle is as small as 30%. In our ABI, the functions of both optical field splitting and phase dithering [19] are carried out by using the single device of AOM. Thanks to this simplification in optical setup, the optical efficiency of the interferometer is as high as $(95 \pm 1)\%$, and can be further improved in principle since it is only confined by the intrinsic loss of the AOMs. When the ABI functions as a high efficiency optical switch for quantum state, only about 50% AOM diffraction efficiency is needed. Therefore, our scheme has the merits of achieving high efficiency with less demanding for AOM driving. Besides, we show the ABI we realized can be used to

^{*} xueshiguo@tju.edu.cn

[†] xiaoyingli@tju.edu.cn

coherently combine two optical quantum states with small optical frequency difference. The high efficiency switching and the coherent combination capacity of our ABI scheme make it a powerful tool for quantum technology and are useful for the generation of entangled quantum state [20].

II. EXPERIMENTAL PRINCIPLE

We first illustrate the working principle of the ABI. As shown in Fig.1(a), when two optical fields \hat{a}_{ω_1} and \hat{b}_{ω_2} satisfying the standard bosonic commutation relation $[\hat{a}_{\omega_1}, \hat{a}_{\omega_1}^\dagger] = [\hat{b}_{\omega_2}, \hat{b}_{\omega_2}^\dagger] = 1$ are aligned to the -1^{st} order and the $+1^{st}$ order of Bragg diffraction of an AOM with driving frequency of Ω , the output fields \hat{c} and \hat{d} have the form of [12]

$$\begin{aligned}\hat{c} &= t\hat{b}_{\omega_2} + e^{i\theta}r\hat{a}_{\omega_1-\Omega} \\ \hat{d} &= t\hat{a}_{\omega_1} - e^{-i\theta}r\hat{b}_{\omega_2+\Omega},\end{aligned}\quad (1)$$

where t, r are the splitting parameters and θ is AOM induced phase. In general, each output port contains optical fields with two different frequencies. However, in the particular case of $\omega_1 = \omega + \Omega$ and $\omega_2 = \omega$, the two split optical modes from an AOM only contains the optical field with frequency ω and $\omega + \Omega$. Following the idea of combining

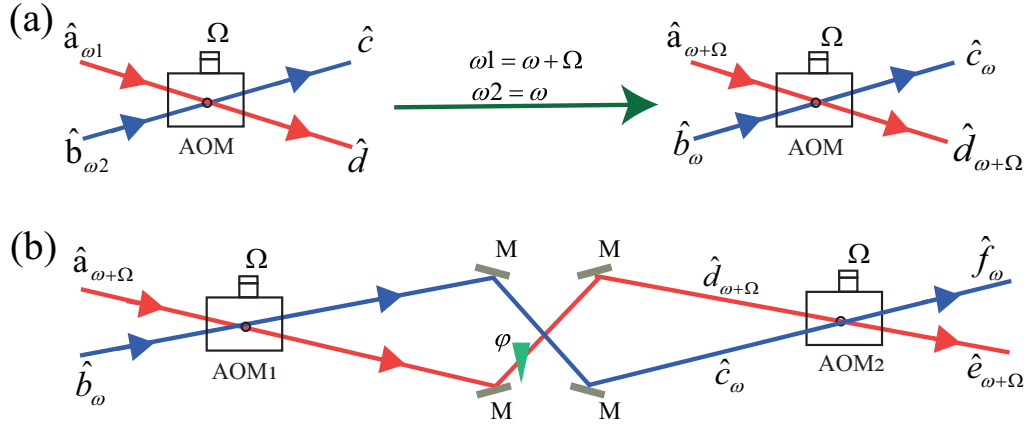


FIG. 1. (a) The optical frequency shifting property when an acousto-optic modulator (AOM) is used as a bi-frequency beam splitter/combiner. (b) An AOM based bi-frequency interferometer (ABI) whose output ports preserve the optical frequency at the output ports.

the same optical frequency in the same spatial mode, we propose an ABI as Fig.1(b), where the both input fields are diffracted twice with different directions of frequency shifting. For input fields $\hat{a}_{\omega+\Omega}$ and \hat{b}_{ω} with optical frequency $\omega + \Omega$ and ω , the output optical fields of the interferometer can be obtained by using Eq. (1) twice:

$$\begin{aligned}\hat{e}_{\omega+\Omega} &= [t_1 t_2 e^{i\varphi} - r_1 r_2 e^{i(\theta_1 - \theta_2)}] \hat{a}_{\omega+\Omega} - \\ &\quad [r_1 t_2 e^{i(\varphi - \theta_1)} + t_1 r_2 e^{-i\theta_2}] \hat{b}_{\omega+\Omega} \\ \hat{f}_{\omega} &= [r_1 t_2 e^{i\theta_1} + t_1 r_2 e^{i(\theta_2 + \varphi)}] \hat{a}_{\omega} + \\ &\quad [t_1 t_2 - r_1 r_2 e^{i(\theta_2 - \theta_1 + \varphi)}] \hat{b}_{\omega},\end{aligned}\quad (2)$$

where φ is the phase difference between the two arms of the ABI, $t_{1,2}$, $r_{1,2}$ and $\theta_{1,2}$ are the splitting parameters and acoustic modulation induced phase of AOM₁ and AOM₂, respectively.

III. APPLICATIONS IN QUANTUM TECHNOLOGY

The ABI in Fig.1(b) can function as a bi-frequency beam-splitter for input fields $\hat{a}_{\omega+\Omega}$ and \hat{b}_{ω} with arbitrary splitting ratio. According to Eq.(2), two input fields $\hat{a}_{\omega+\Omega}$ and \hat{b}_{ω} can be splitted with desired total splitting parameters ratio t' and r' , as shown in Fig.2(a), if the AOM splitting parameters are set to $t_{1(2)}^2 = r_{1(2)}^2 = 0.5$ and the phase parameters can be arbitrarily controlled. With this feature in mind, we discuss the specific application of the ABI in quantum

technology as a high efficiency and high isolation optical switch as illustrated in Fig.2(b). When the RF signal is completely shut down, the optical path of the interferometer is degraded into two independent propagated spatial modes. Imagine a quantum state $|\psi\rangle_\omega$ with optical frequency ω is send to \hat{b}_ω input port of the ABI at Fig.1(b) and the other input port is reserved to the vacuum state, the quantum state goes through the "off port" shown in Fig.2(b) without any interaction and the "on port" is in a high isolation level to the quantum state. On the other hand, when the RF signal is on, the quantum state will be divided into both the "off port" and the "on port" in general depending on the splitting ratio of the two AOMs and the phase difference between the interference process. If we set the overall splitting ratio of the ABI in Fig.2(a) to $t' = 0$ and $r' = 1$ by controlling the phase, the quantum optical state is transmitted to "on port" up to a optical frequency shift and with high transmitting efficiency. Depending on the specific quantum application, the frequency shift can have different influence. For example, when the ABI is used as a switch before photon detector, the frequency within RF range is usually irrelevant since the response difference for optical power detector with respect to the tiny frequency difference is negligible. However, when the quantum state is detected with a coherent detection scheme such as homodyne detection, this frequency shift will affect the output of the detection scheme. On one hand, this may require us to carefully compensate the frequency shift to get a stable output signal in regular coherent detection schemes. On the other hand, this controllable frequency shift also provide us a handy tool to realize quantum state frequency tuning for coherent detection schemes with local references [21].

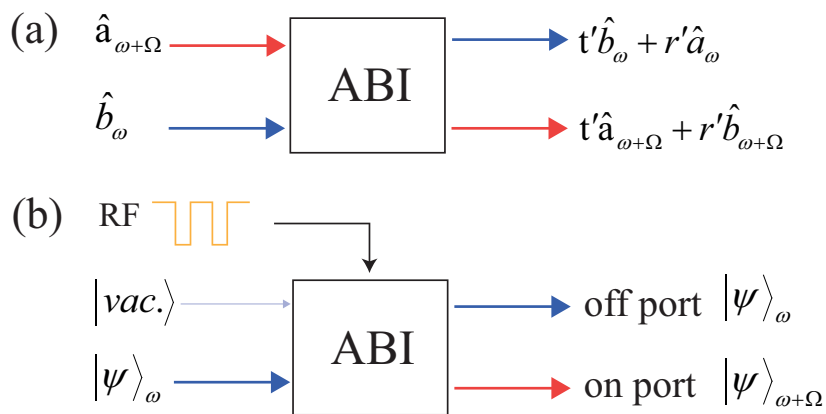


FIG. 2. (a) AOM based bi-frequency interferometer (ABI) as a variable bi-frequency beam splitter. (b) With chopped RF driving signal, ABI functions as a high efficiency high isolation optical switch.

Besides the optical switch application we discussed above, the bi-frequency beam splitting property of the ABI can also be used to coherently combine two quantum state, which is a crucial operation in entanglement generation [20, 22, 23]. Different from the regular scheme that combines two optical fields with the same optical frequency by using linear beam-splitters, our scheme coherently combines two optical fields with different frequencies. Since frequency is one of the import degree of freedoms for quantum optical mode [24], possible applications with this scheme can be creating frequency entangled photon pairs out of two single photons, creating continuous variable Einstein-Podolsky-Rosen state out of two single mode squeezing state with frequency difference or create a large scale entangled state with multiple pairs of frequency encoded two mode entangled states [20, 22, 23].

IV. EXPERIMENTAL SETUP AND RESULT

Our experimental setup for demonstrating acousto-optic modulator based bi-frequency interferometer is shown in Fig.3(a). A linearly polarized optical field at 1550 nm band, prepared by passing a narrow line width laser through a polarization beam-splitter (PBS), is coupled to the +1st Bragg mode. When the driving RF signal of AOM₁ is on, the injected optical field is splitted into a frequency up-shifted arm (red line) and a non-shifted arm (blue line). For each arm, two plane mirrors and a concave mirror (CM) with 300 mm radius of curvature are used to guide the laser beam to the AOM₂. The spatial mode matching of the interference at AOM₂ is optimized by carefully tuning the position of the CMs. To control the phase between two arms and realize phase locking, a piezo device (PZT) is mounted on the concave mirror of the frequency shifted arm. At the output of the AOM₂, the intensity of the frequency up-shifted port is detected by a photo diode (PD). Since the intensity summation of the two output ports is an invariant, the intensity at the other port can be deduced accordingly and is not presented in the paper. By tuning the power of RF signals applied to AOM₁ and AOM₂, the splitting ratio of the AOM is set to be $t_{1,2}^2 = r_{1,2}^2 = 0.5$. Modeling the input

light as a coherent state $|\alpha\rangle$, the ideal output intensity of the ABI system can be obtained by using Eq. (2)

$$I_{out} = \langle \alpha | \hat{e}_{\omega+\Omega}^\dagger \hat{e}_{\omega+\Omega} | \alpha \rangle = \frac{1}{2} [1 + \cos(\phi)] I_{in}, \quad (3)$$

where $\phi = \varphi - \theta_1 + \theta_2$ is the phase difference between two arms, $I_{in} = |\alpha|^2$ is the intensity of the input light. In the experiment, we consider three practical parameters: (i) the non-ideal efficiency η of the optical components, (ii) the mode mis-matching induced non-ideal visibility V of the interference, and (iii) the beat between the two RF driving signals. With these parameters considered, Eq. (3) is rewritten as

$$I'_{out} = \frac{\eta}{2} [1 + V \cos(\Delta\omega T + \phi)] I_{in}, \quad (4)$$

where $\Delta\omega$ is the angular frequency difference of the RF signals and T is the time variable.

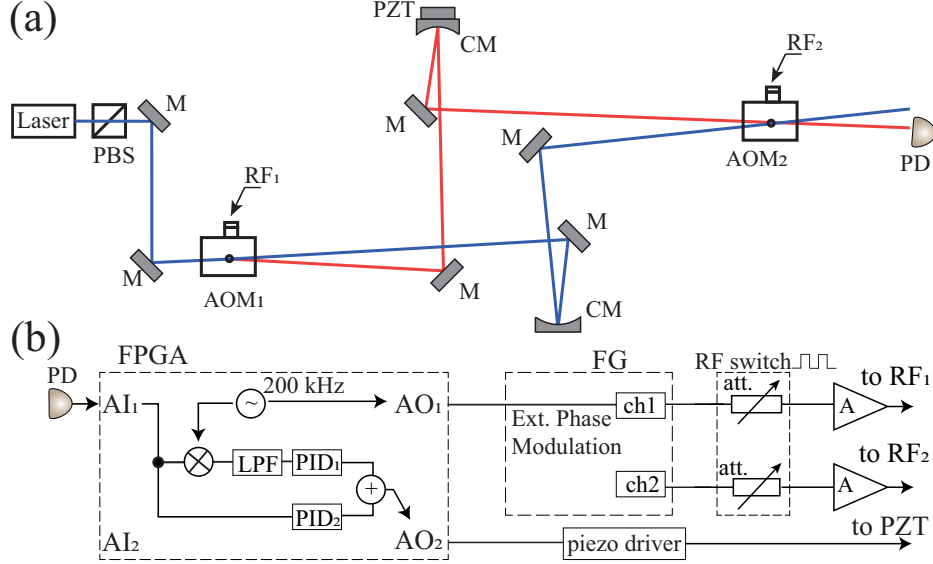


FIG. 3. (a) The experimental setup of the AOM based bi-frequency interferometer. (b) The diagram of the electronic circuits used to drive the two AOMs and the PZT. PBS, polarization beam splitter; AOM, Acousto-optic modulator; CM, concave mirror; M, plane mirror; PZT, piezo-electric translation device; PD, photo diode. LPF: low pass filter; AI_{1,2}: analog input, AO_{1,2}: analog output, FG: function generator, att.: voltage controlled attenuator, A: amplifier.

The detailed electrical circuits for driving and controlling the ABI is shown in Fig.3(b). The RF signals RF₁ and RF₂ are generated by a two channel arbitrary function generator (SIGLENT-SDG2122X) and further amplified by amplifiers. Two voltage controlled attenuators at the input port of the RF amplifiers are used to adjust the splitting ratio of the AOMs, and they can also cut off the AOMs driving RF signals in real time. With the help of proper electronic amplifiers and AD/DA converters, the driving signal sending to the PZT driver in Fig.3(b) is controlled in real time by a FPGA system (STEMLab125-14) with two analog inputs and two analog outputs, which also records the intensity information from the PD. To stably lock the ABI to arbitrary working point of phase, it is necessary to introduce some phase dithering to one of the two arms of ABI [19]. Here we realize this by adding a 200 kHz phase modulation with a small modulation depth to RF₁. By doing this, the phase dithering function is also integrated into AOM₁, and no extra optical component for phase dithering generation is necessary. With the above mentioned hardware, the working phase of the ABI can be locked by properly configure the FPGA system. Here we use PyRPL phase locking package [25] to achieve this, and the simplified schematics of the FPGA system are shown in the dashed square labeled with FPGA in Fig.3(b). The digital signal of the ABI intensity is down mixed at 200 kHz, and the direct pass and the down mixed signal is sent to two PIDs with different parameters. The output of the PIDs are combined and sent to the piezo driver through the analog output port of the FPGA.

During the experiment, we measure the intensity I'_{out} at one output in different cases, and the main results are shown in Fig.4. In order to analyze the results conveniently, I'_{out} is normalized to the intensity of input field I_{in} . Firstly, we demonstrate the beating signal, and calibrate the visibility of the interference V and the optical efficiency η by fitting the data to Eq. (4). The frequency of the signal RF1 and RF2 are 80 MHz and 79.9 MHz, and thus the beat frequency $\Delta\omega/2\pi$ is set to 100 kHz. The directly measured beating signal and the fitting are respectively represented

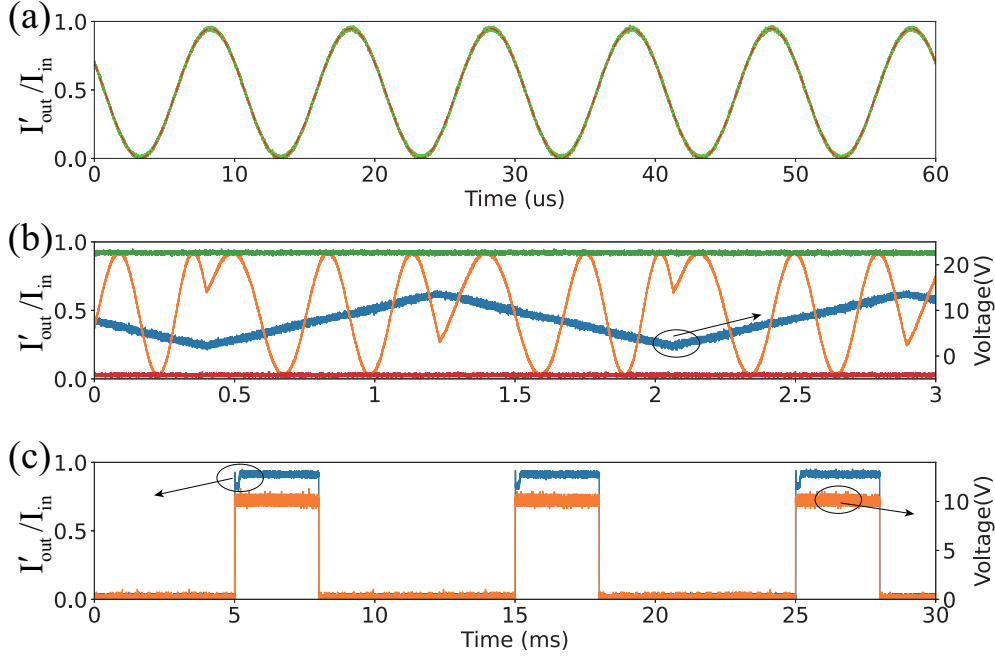


FIG. 4. Experimental result. (a) Beating signal when two AOMs are driving in a RF frequency difference of 100 kHz: green trace, directly measured beat signal; red dash-dotted line, fitting of the beating signal. (b) Single port output intensity of an ABI in continuous driving mode; (c) Single port output intensity of an ABI in chopped phase locking mode with a locking duty cycle of 30%.

by the green trace and red dash-dotted lines in Fig.4(a). The fitting curve overlaps well with the directly measured data, and the result of the fitting parameters in Eq(4) are $V=(99.5 \pm 0.2)\%$, $\eta=(95 \pm 1)\%$ and $\phi=(1.08 \pm 0.01)$ rad, respectively. This beating result is similar to that presented in [12], but here we greatly enhance the visibility to an almost perfect level and realize a high optical efficiency meanwhile. We note each optical surface in our setup has a loss of about 0.5% limited by the quality of optical coating, so η can be further improved once components with better optical coatings are used.

In the next, we set RF_1 and RF_2 to be identical frequency of 80 MHz. By scanning the PZT with a ramp signal (blue trace in Fig.4(b)), we observe the interference fringe, as is shown by the orange trace of Fig.4(b). When triggered by the ramp (blue trace), one sees the fringe moves on the oscilloscope horizontally caused by the phase drift between the two arms. This drift can be stabilized by our phase locking circuits. The green and red traces in Fig.4(b) are obtained when the ABI is respectively locked to the maximum and minimum output working point. Compared Fig.4(b) to Fig.4(a), we find the visibility of interference for the identical frequency case is reduced to $(93.7 \pm 0.5)\%$. Fitting the data by using Eq. (4), we find, the total transmission efficiency of the ABI when used as a optical switch is $(92 \pm 1.1)\%$. We study the reason for this visibility reduction and find, besides a phase shift, the PZT can cause the beam walking-off and will therefore induce mode mis-matching. This indicates the visibility in identical frequency driving mode can be further optimized by removing the PZT and introducing phase shift by AOM_2 in Fig.3(a). To complete this optimization, angle calculation and phase unwrapping algorithms is necessary to be implemented in the FPGA [21] and the progress is underway.

We further demonstrate the chopped locking mode of the ABI, and the result is shown in Fig.4(c). In this specific working mode, a 100 Hz electronic gate pulses (shown in Fig.4(c) by the orange trace) are applied to the voltage controlled attenuators in Fig.3(b). When the gate signals are in high voltage, the whole system works the same as ABI being locked at the maximum output (green trace in Fig.4(b)). When the gate signals is low, the driving signal of the two AOMs in the ABI is cut off, and the injected light will go through the non-shifted arm (blue line) in Fig.3(a) and the power I_{out} is zero. In our system, the gate pulse is also sent to the PID block of the FPGA to keep the PID output value unchanged when the optical interference structure is destroyed. As it is shown in Fig.4(c), with the help of passive phase stabilization approach, our ABI can work with a duty cycle as low as 30%.

Finally, we analyze the isolation property of the ABI when it is used as an optical switch. We couple only a small fraction of the free space light from the frequency up-shifted output port of AOM_2 into a fiber coupled single photon detector (id Quantique-id200) working at gated mode of 1 MHz triggers per second. Since the isolation of the

ABI functions as an optical switch is large enough to exceed the dynamic range of the SPD, we respectively insert calibrated optical attenuators of 102 dB and 22 dB when measuring the photon numbers of switching on state and switching off state. By comparing the photon counting result for the two cases, we find the isolation of our system is about 74 dB, which shows the ABI can function as a high isolation optical switch.

V. SUMMARY

In summary, we experimentally realized an AOM based bi-frequency interferometer. The interference visibility of the beating signal of the ABI is $(99.5 \pm 0.2)\%$ and an optical efficiency is $(95 \pm 1)\%$, which make the system suitable for high efficiency quantum technology. When the ABI is properly controlled and operated as an optical switch, our system has a overall quantum efficiency of $(92 \pm 1.1)\%$ and the isolation is about 74 dB. The ABI can stably work in chopped phase locking mode with a locking duty cycle as low as 30%, and functions of both dithering generation for the phase locking and optical field splitting are realized in one AOM. Besides, our analysis shows the ABI can be applied to the coherent combination of optical state with different optical frequencies and quantum entanglement generation. The performance of experimental system we realized is currently confined by the optical loss of the components and the beam walk-off induced by the PZT. With the high visibility of the beating signal, we believe the overall efficiency to implement optical switching or coherently combining of quantum states with the ABI we proposed can be further improved to around 98%-99% with commercially available ultra-low loss optical components.

ACKNOWLEDGMENTS

This work was supported in part by National Natural Science Foundation of China (Grants No. 12004279).

-
- [1] G. Wade, Bulk-wave acousto-optic bragg diffraction, in *Guided-Wave Acousto-Optics: Interactions, Devices, and Applications*, edited by C. S. Tsai (Springer Berlin Heidelberg, Berlin, Heidelberg, 1990) pp. 11–52.
 - [2] F. Tricot, D. H. Phung, M. Lours, S. Guérandel, and E. de Clercq, Power stabilization of a diode laser with an acousto-optic modulator, *Review of Scientific Instruments* **89**, 113112 (2018).
 - [3] J. Dong, Y. Hu, J. Huang, M. Ye, Q. Qu, T. Li, and L. Liu, Subhertz linewidth laser by locking to a fiber delay line, *Appl. Opt.* **54**, 1152 (2015).
 - [4] E. Song, T. Dai, G. Zhu, H. Wang, K. Aleksei, and X. Zhu, Adjustable and stable beam profile generation in a yb:yag thin-disk laser, *Opt. Lett.* **45**, 6550 (2020).
 - [5] R. Bola, D. Treptow, A. Marzoa, M. Montes-Usategui, and E. Martín-Badosa, Acousto-holographic optical tweezers, *Opt. Lett.* **45**, 2938 (2020).
 - [6] O. de Vries, T. Saule, M. Plötner, F. Lücking, T. Eidam, A. Hoffmann, A. Klenke, S. Hädrich, J. Limpert, S. Holzberger, T. Schreiber, R. Eberhardt, I. Pupeza, and A. Tünnermann, Acousto-optic pulse picking scheme with carrier-frequency-to-pulse-repetition-rate synchronization, *Opt. Express* **23**, 19586 (2015).
 - [7] K. Takase, A. Kawasaki, B. K. Jeong, M. Endo, T. Kashiwazaki, T. Kazama, K. Enbutsu, K. Watanabe, T. Umeki, S. Miki, H. Terai, M. Yabuno, F. China, W. Asavanant, J. ichi Yoshikawa, and A. Furusawa, Generation of schrödinger cat states with wigner negativity using a continuous-wave low-loss waveguide optical parametric amplifier, *Opt. Express* **30**, 14161 (2022).
 - [8] A. Kawasaki, K. Takase, T. Nomura, S. Miki, H. Terai, M. Yabuno, F. China, W. Asavanant, M. Endo, J. ichi Yoshikawa, and A. Furusawa, Generation of highly pure single-photon state at telecommunication wavelength, *Opt. Express* **30**, 24831 (2022).
 - [9] J. Appel, E. Figueroa, D. Korystov, M. Lobino, and A. I. Lvovsky, Quantum memory for squeezed light, *Phys. Rev. Lett.* **100**, 093602 (2008).
 - [10] V. Michaud-Belleau, J.-D. Deschênes, and J. Genest, Reaching the true shot-noise-limited phase sensitivity in self-heterodyne interferometry, *IEEE Journal of Quantum Electronics* **58**, 1 (2022).
 - [11] Y. Okawa, F. Omura, Y. Yasutake, and S. Fukatsu, Photon heterodyning, *Opt. Express* **25**, 20156 (2017).
 - [12] R. Mathevet, B. Chalopin, and S. Massenot, Single photon beat note in an acousto-optic modulator-based interferometer, *American Journal of Physics* **88**, 313 (2020).
 - [13] J. Arnbak, C. S. Jacobsen, R. B. Andrade, X. Guo, J. S. Neergaard-Nielsen, U. L. Andersen, and T. Gehring, Compact, low-threshold squeezed light source, *Opt. Express* **27**, 37877 (2019).
 - [14] C.-H. Chang, R. K. Heilmann, M. L. Schattenburg, and P. Glenn, Design of a double-pass shear mode acousto-optic modulator, *Review of Scientific Instruments* **79**, 033104 (2008).
 - [15] W. J. Schwenger and J. M. Higbie, High-speed acousto-optic shutter with no optical frequency shift, *Review of Scientific Instruments* **83**, 083110 (2012).

- [16] X. Ma, X. Zhang, K. Huang, and X. Lu, Noise-suppressing and lock-free optical interferometer for cold atom experiments, *Opt. Express* **28**, 28584 (2020).
- [17] M. M. de Lima, M. Beck, R. Hey, and P. V. Santos, Compact mach-zehnder acousto-optic modulator, *Applied Physics Letters* **89**, 121104 (2006).
- [18] F. Herzog, K. Kudielka, D. Erni, and W. Bachtold, Optical phase locking by local oscillator phase dithering, *IEEE Journal of Quantum Electronics* **42**, 973 (2006).
- [19] S. Wu, W. Huang, P. Yang, S. Liu, and L. Chen, Arbitrary phase-locking in mach-zehnder interferometer, *Optics Communications* **442**, 148 (2019).
- [20] M. V. Larsen, X. Guo, C. R. Breum, J. S. Neergaard-Nielsen, and U. L. Andersen, Fiber-coupled epr-state generation using a single temporally multiplexed squeezed light source, *npj Quantum Information* **5**, 46 (2019).
- [21] I. Suleiman, J. A. H. Nielsen, X. Guo, N. Jain, J. Neergaard-Nielsen, T. Gehring, and U. L. Andersen, 40 km fiber transmission of squeezed light measured with a real local oscillator, *Quantum Science and Technology* **7**, 045003 (2022).
- [22] J.-i. Yoshikawa, S. Yokoyama, T. Kaji, C. Sornphiphatphong, Y. Shiozawa, K. Makino, and A. Furusawa, Invited article: Generation of one-million-mode continuous-variable cluster state by unlimited time-domain multiplexing, *APL Photonics* **1**, 060801 (2016).
- [23] W. Asavanant, Y. Shiozawa, S. Yokoyama, B. Charoensombutamon, H. Emura, R. N. Alexander, S. Takeda, J. ichi Yoshikawa, N. C. Menicucci, H. Yonezawa, and A. Furusawa, Generation of time-domain-multiplexed two-dimensional cluster state, *Science* **366**, 373 (2019).
- [24] M. Chen, N. C. Menicucci, and O. Pfister, Experimental realization of multipartite entanglement of 60 modes of a quantum optical frequency comb, *Phys. Rev. Lett.* **112**, 120505 (2014).
- [25] L. Neuhaus, R. Metzдорff, S. Chua, T. Jacqmin, T. Briant, A. Heidmann, P.-F. Cohadon, and S. Deléglise, Pyrpl (python red pitaya lockbox) - an open-source software package for fpga-controlled quantum optics experiments, *2017 European Conference on Lasers and Electro-Optics and European Quantum Electronics Conference*, 2017 European Conference on Lasers and Electro-Optics and European Quantum Electronics Conference , EA_P_8 (2017).